Generation of SHG Holograms at 400 nm from a Beam-Shaped Fundamental Using Short Femtosecond Pulses in a Collinear Type-2 Phase Matching Crystal

Alexander Romboy*[1,2], Kristian Cvecek[1,2], and Michael Schmidt[1,2]

[1]*Institute of Photonic Technologies, Friedrich-Alexander-Universität Erlangen-Nürnberg, Konrad-Zuse-Str.3/5, 91052 Erlangen, Germany*

[2]*Erlangen Graduate School in Advanced Optical Technologies (SAOT), Friedrich-Alexander-Universität Erlangen-Nürnberg, Konrad-Zuse-Str.3/5, 90152 Erlangen, Germany*

**Corresponding author's e-mail: alexander.romboy@lpt.uni-erlangen.de*

The feasibility of using beam shaped short femtosecond pulses in combination with a nonlinear frequency conversion process to create any arbitrary beam shape in the ultraviolet spectrum is shown. Broadband femtosecond pulses (800 nm centre, 30 nm Bandwidth FWHM, 50 fs) are shaped via a spatial light modulator (SLM) and converted to 400 nm in a subsequent second harmonic process to 400 nm in a collinear setup while conserving the beam shape information by using orthogonal polarisation states to avoid beam shape degradation. Additionally, it is shown, that the holograms exhibit blurred edges due to chromatic dispersion stemming from the bandwidth of the utilized fs pulses and the conversion efficiency is linked to the angular spectrum created at the SLM.

DOI: 10.2961/jlmn.2026.01.2006

Keywords: beam shaping, femtosecond, second harmonic generation, spatial light modulator, nonlinear optics, computed generated holography

1. Introduction

The benefits of beam shaping have found entry into various domains of laser materials processing: Spatial beam shaping for e.g., hole drilling with ultrashort laser pulses to increase ablation efficiency, temporal beam shaping to tailor the temporal irradiation of a sample with ultrashort pulses or other modalities of beam shaping, such as polarization shaping, angular orbital momentum shaping and so on [1]. One technique for beam shaping uses the wave properties of light e.g., in diffractive optics. These excel in their high degree of freedom in the resulting beam shape. Especially dynamic beam shaping is of interest for laser machining applications, such as surface structuring, since it allows adjustment of the beam shape in real time and thus the ablation profile during the machining process [2]. Liquid Crystal on Silicon - Spatial Light Modulators (LCoS-SLMs) do offer both these advantages. Because of this, SLMs have become a centrepoint of attention in research for laser materials processing and sensing applications [3].

LCoS-SLMs, as their name implies, are based on liquid crystal pixels, where the refractive index can be modulated individually. This in turn is used to locally delay an incoming wave front and as a result alter the beam shape [4].

In addition to beam shaping, requirements for higher processing and imaging resolutions have pushed for more research in the ultraviolet (UV) spectrum. UV wavelengths allow for smaller focal spots and improved resolutions in microscopy. In laser material processing, another advantage is the improved productivity for certain materials e.g. polymers [5]. The photon energy of UV radiation is able to break the chemical bonds directly and is able to ablate the material without introducing excess heat into the process. Especially beam shaped UV-laser beams are of interest for applications like structured illumination microscopy and selective ablation of heat sensitive coatings like amorphous carbon coatings on steel, since these applications require a specific beam shape to enable the method or achieve optimal efficiency respectively [6, 7].

Recent advances in nonlinear metamaterials enable dynamic beam shaping at various wavelengths, including UV, [8, 9] or at very high frame rates [10]. While they offer much higher nonlinear susceptibilities compared to bulk crystals [11], due to their physical length, the overall efficiency is still lower than the latter, necessary for industrial laser machining applications.

Laser written nonlinear crystals (e.g. lithium niobate) crystals offer higher conversion efficiencies and even dynamic beam shaping through input wavelength or polarisation modulation, although they are still limited in the dynamically achievable beam shapes [12, 13].

LCoS-SLMs are available for most wavelengths in the visible and infrared (IR) range but not for ultraviolet wavelengths (typically stopping at around 400 nm), since the liquid crystals start absorbing in the UV wavelength. To overcome this limitation, one can employ a nonlinear process to

frequency convert a shaped fundamental beam from the visible or IR range into the UV spectrum while maintaining the beam shaping information.

As shown by Won et. al., femtosecond (fs) pulses at 800 nm fundamental, that were beam shaped by an SLM, can be frequency converted into 400 nm and 266 nm through second and third harmonic generation (SHG and THG) respectively, while retaining the beam shaping information. The authors utilized a non-collinear type-1 phase matching setup. This is necessary, because nonlinear beam shaping requires a non-degenerate frequency conversion process, to not degrade the holograms through interangular mixing. The non-collinear setup limits the achievable conversion efficiency – in this case 1.0×10^{-3} % for SHG using a quartz crystal as the nonlinear medium [14]. An alternative non-degenerate SHG-process is a collinear Type-2 setup, which offers higher conversion efficiencies and a simpler optical setup, as shown by Ackerman et al. The authors created SHG Holograms at 532 nm, also using an SLM to beam shape picosecond pulses at 1064 nm fundamental in a collinear Type-2 phase matching setup – the conversion efficiencies were up to 33% using a 9 mm long KTP crystal [15].

This paper aims to show the viability of the collinear Type-2 setup also for shorter pulses by transferring it to use with fs pulses for the advantages listed above. Since fs pulses typically offer higher intensities than ps pulses, a few considerations need to be taken into account: Firstly, shorter crystals should be used, because they offer higher angular acceptance for larger holograms, while maintaining higher conversion efficiency due to a smaller accumulated phase matching mismatch. Secondly, non-linear effects that occur in the intermediate focus of the setup, like Super Continuum Generation, can be detrimental for the SHG process. Additionally, effects that are expected to occur with the utilization of pulses with a large spectral bandwidth (in this case 30 nm bandwidth FWHM), like chromatic dispersion, will be highlighted.

2. Theoretical background

Nonlinear frequency conversion processes revolve around one condition: Phase matching. This means that the sum of wavevectors of the fundamental waves and wave vector of the harmonic wave match. The difference of those wave vectors is called the phase mismatch Δk (Eq.1) [16] and needs to be minimized to achieve a high conversion efficiency.

$$\Delta k = k_1 + k_2 - k_3. \quad (1)$$

This is usually achieved by using birefringent nonlinear crystals and tuning the incidence angle of the beam into the crystal such that the refractive indices for the fundamental and harmonic frequencies are equal. For plane waves, there is only one propagation direction that needs to be taken into account.

Since an LCoS-SLM acts on the phase of an incoming light field, it alters the wave front and with that, introduces new propagation directions – an angular spectrum A (Eq. 2). This can be analysed by Fourier Transformation of the shaped complex light field U. Additionally, since the "normal" Fourier Transform only provides spatial frequencies, the projection of plane waves with a certain wavelength λ at different propagation angles is equated to the spatial frequencies in the observation plane [17, 18].

$$A\left(\frac{\alpha}{\lambda},\frac{\beta}{\lambda};z\right) = \iint_{-\infty}^{\infty} U(x,y,z)e^{-i2\pi\left(\frac{\alpha}{\lambda}x+\frac{\beta}{\lambda}y\right)}\,dx\,dy. \quad (2)$$

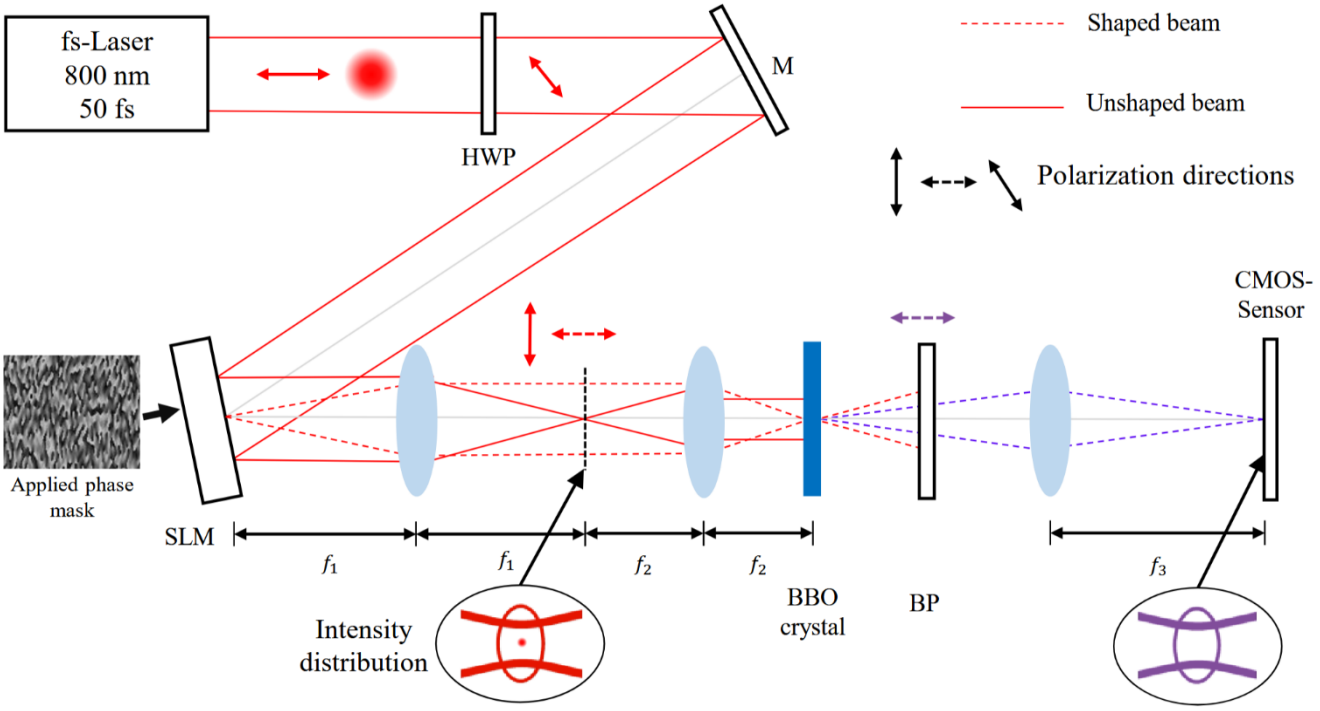

Fig. 1: Experimental setup for non-linear holography
(HWP: Half Wave Plate; M: Mirror; SLM: Spatial Light Modulator; BP: Bandpass filter).

These additional propagation directions in a shaped beam have an impact on the phase matching since the larger the deviation from the ideal propagation direction becomes the higher the phase mismatch and thus the lower the expected conversion efficiency. This can be compensated for by using thin non-linear crystals, because the overall accumulated is depended on the length L of the crystal and follows a sinc function (Eq. 3). Thus, they can more uniformly frequency convert a large angular spectrum [16].

$$I_{Harmonic} = I_{Harmonic}^{(max)} \left[\frac{\sin\left(\frac{\Delta kL}{2}\right)}{\frac{\Delta kL}{2}} \right]^2 . \quad (3)$$

3. Methods and experimental setup

The experimental setup (Fig. 1) can be subdivided into two parts: Beam shaping via SLM and Second Harmonic Generation via a non-linear crystal. the beam from a Femtosecond Laser (Coherent Astrella USP-1k, 800 nm, 1 kHz) is attenuated by using the primary reflection of a wedged plate and cropped to 15 mm by an aperture to ensure full illumination of the SLM while avoiding uncontrolled cropping on other components due to clear aperture limitations. Its polarization direction is rotated by 45° by a half-wave-plate. This diagonal polarization state can also be seen as an even superposition of horizontal and vertical polarizations. Since the SLM (Hamamatsu X15213-02R; resolution 1272x1024 px; 12.5 µm pixel pitch) is only capable of shaping the horizontal component of the incident beam, it is subdivided into a shaped component and an unshaped component. Both are imaged onto a non-linear crystal (β-BBO; 0.1mm thick; Eksma Optics) through a 4f-imaging-setup with a demagnification of m = 0.5 (f1 = 300 mm; f2 = 150 mm). The crystal is cut for Type 2 phase matching. This means that the three-wave-mixing (TWM) process can occur only between two orthogonally polarized photons, which in this setup means that TWM only occurs between a “shaped” and an “unshaped” photon. In this way the shaped horizontally polarized partial beam effectively becomes a signal, since it contains the shaped wavefront information and the unshaped collimated beam becomes a pump to supply the energy to frequency convert the shaped signal into a shorter wavelength. Additionally, this avoids the mixing of shaped photons with one another, which would significantly degrade the desired intensity distribution of the beam.

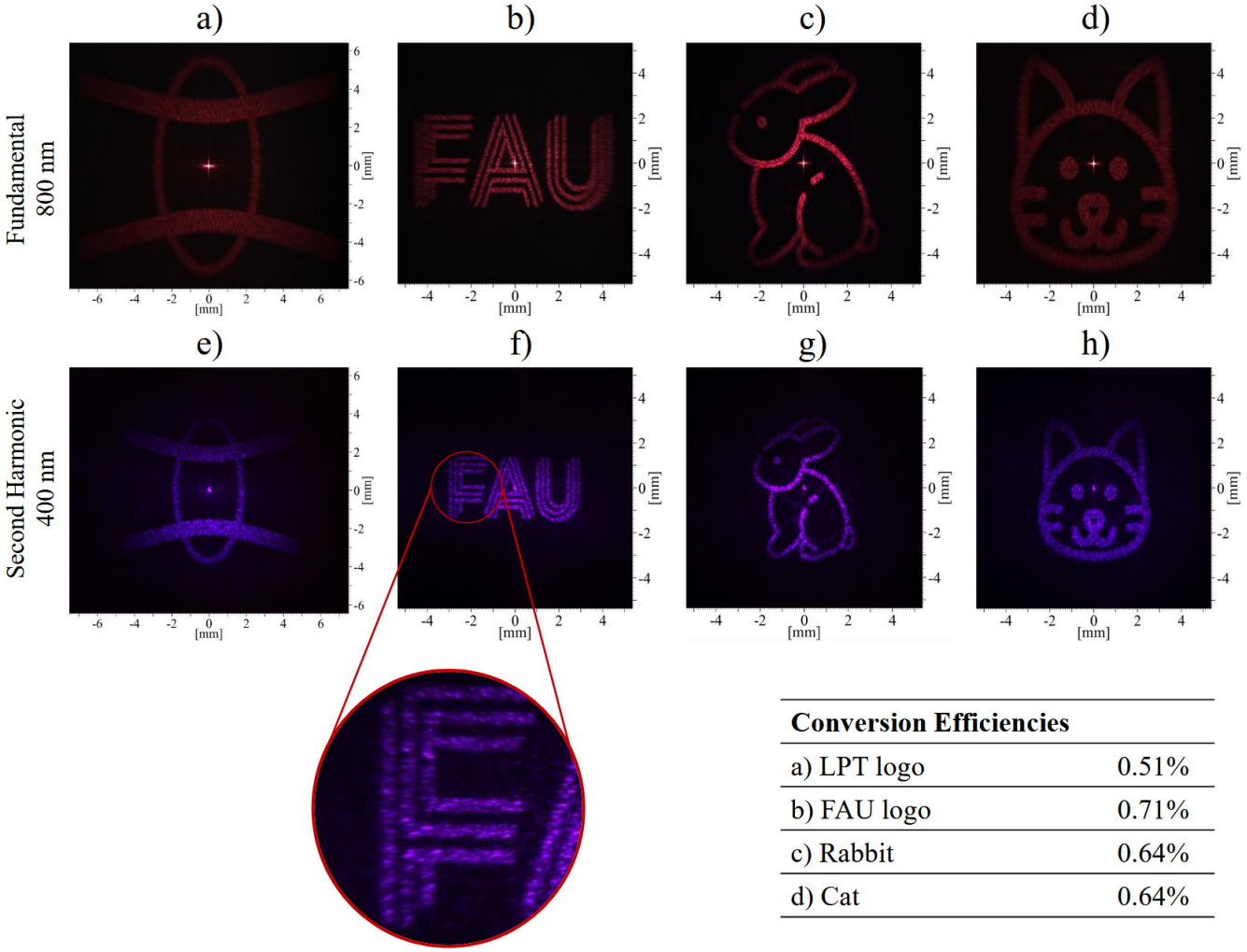

Conversion Efficiencies	
a) LPT logo	0.51%
b) FAU logo	0.71%
c) Rabbit	0.64%
d) Cat	0.64%

Fig. 2: Holograms shaped in the fundamental at 800nm (a-d), and in the second harmonic at 400 nm (e-h). In the highlighted section the radial blur can be seen.

Afterwards, the fundamental wavelength is blocked via a bandpass filter (Thorlabs FBH400-40) and the UV-hologram is imaged onto a CMOS-Sensor (Canon EOS 550D, 22.3 x 14.9 mm^2 sensor size) via a lens (Thorlabs LA4102-UV, f = 200 mm). Additionally, power measurements were taken before the non-linear crystal and after the bandpass filter to measure the conversion efficiency.

Table 1: Used laser parameters.

Pulse duration (FWHM)	50 fs
Pulse energy	787 µJ
Beam diameter after aperture	15 mm

Phase mask calculation was performed using an iterative algorithm on the basis of Gerchberg-Saxton [19]. Power measurements were taken with the power meters Coherent PM10 and Coherent PS19Q. Spectral measurements were taken with an OceanOptics HR6 spectrometer.

4. Results and Discussion

As can be seen in Fig. 2e-h, the desired beam shape has been carried over into the second harmonic beam with high uniformity. The corner regions of larger holograms as in Fig. 2e experience lower conversion efficiency, since the size of a hologram is directly linked with a larger angular spectrum and thus an increase in phase mismatch – though, the angular spectrum can be scaled with lenses of different focal lengths in the setup. However, the edges of the holograms are blurred from the centre outward, due to chromatic dispersion stemming from the spectral bandwidth of the pulse and a grating effect on the SLM [20]. This can be seen in the fundamental holograms, as well as in the second harmonic. This limits the effective size of the holograms, since edges far away from the centre cannot be resolved sharply.

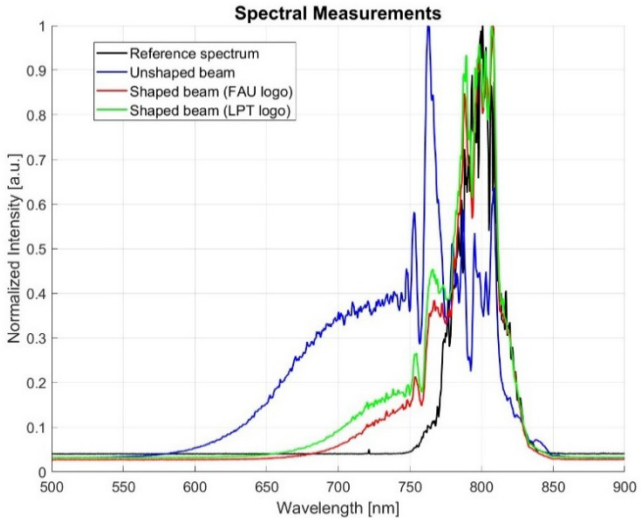

Fig. 3: Spectral measurement of the supercontinuum, created in the intermediate focus of the 4f-optic at different beam shapes: black: Reference spectrum without supercontinuum generation; blue: focused plane wave without beam shaping; green Shaped beam with Fig. 2a intensity distribution; red: Shaped beam with Fig. 2b intensity distribution.

The conversion efficiency for the holograms is between 0.51% and 0.71%. The reference for an unshaped beam in this setup is 1.1%. Although the latter measurement is taken with a Galilean telescope of the same demagnification, because air ionization in the intermediate focus creates a supercontinuum (SC). This prevents a controlled SHG-process, since it shifts energy away from the fundamental frequency into shorter wavelengths (Fig. 3) [20]. This is also the case during beam shaping, because a bit more than half of the pulse energy goes through the intermediate focal spot of the Keplerian telescope (50% of the beam remains unshaped and the undiffracted portion of the shaped beam remain collimated after the SLM). This can be also seen in Fig. 3: Additional frequencies around 760 nm are generated. So also in this case, energy from the fundamental is taken away and thus the intensity at the non-linear crystal is reduced.

5. Conclusion and Outlook

As has been shown, beam shaping via spatial light modulators in conjunction with a frequency conversion process allows for the dynamic modulation of femtosecond pulses in the ultraviolet spectrum. Using Type-2 phase matching and being able to distinguish between shaped and unshaped beams by their polarisations allows for the creation of high-quality holograms while still retaining a simple collinear optical setup. This opens up the possibility for dynamic, high efficiency beam shaping beyond the technical limitations of liquid crystal based optical devices. However, this technique has limitations stemming from the ultrashort pulses used. The spectral bandwidth limits the physical size of the hologram due to chromatic dispersion and the unwanted non-linear effects in the intermediate focus of the imaging optic lower the conversion efficiency of the process. Additional measures need to be taken to mitigate these effects, like using an evacuated 4f-telescope to eliminate air ionization and splitting the pulse into its frequency components before beam shaping and recombining them only in the focal plane. Nevertheless, this process can also be used to create even shorter wavelengths to be able to freely control the beam shapes at those wavelengths.

A further consideration for future research would be the transfer of this method to collinear type-1 phase matching. Though, one would need a way to avoid interangular mixing, since the shaped and unshaped beams would be effectively degenerate, which would deteriorate the desired beam shape. The use of sparse orthogonal encoding, as shown in [21], could be used to control the phase matching conditions inside of the crystal and thus the resulting beam shape.

Funding
Deutsche Forschungsgemeinschaft (SCHM 2115/107-1) and Erlangen Graduate School of Advanced Optical Technologies.

Acknowledgements
The authors gratefully acknowledge funding of the Erlangen Graduate School in Advanced Optical Technologies (SAOT) by the Bavarian State Ministry for Science and Art.

Disclosures
(1) In the experimental process of this work, the authors used the tools “Claude” and “ChatGPT” to assist in programming tasks. After using this tool, the authors reviewed and edited the content as necessary and they take full responsibility for the content of the publication.

(2) The authors declare that there are no conflicts of interest related to this article.

Data availability

Data underlying the results presented in this paper may be obtained from the authors upon reasonable request.

References

[1] M. Schmidt, K. Cvecek, J. Duflou, F. Vollertsen, C.B. Arnold, and M.J. Matthews: CIRP Ann., 73, (2024) 533.
[2] C. Mauclair, B. Najih, V. Comte, F. Bourquard, and M. Delaigue: OES, 0, (2025) 250002.
[3] Y. Yang, A. Forbes, and L. Cao: OES, 2, (2023) 230026.
[4] C. Rosales-Guzmán, and A. Forbes: "How to Shape Light with Spatial Light Modulators" SPIE Spotlights, (2017) p. 5.
[5] U. Quentin, F. Kanal, D. Sutter, and C. Stolzenburg: Proc. SPIE, Vol. 10905, (2019) 109050J.
[6] R. Mincigrucci, E. Paltanin, J.-S. Pelli-Cresi, F. Gala, E. Pontecorvo, L. Foglia, D. de Angelis, D. Fainozzi, A. Gessini, D.S.P. Molina, O. Stranik, F. Wechsler, R. Heintzmann, J. Rothhardt, L. Loetgering, G. Ruocco, F. Bencivenga, and C. Masciovecchio: Opt. exp., 32, (2024) 30813.
[7] T. Häfner: J. Laser Micro. Nanoengin., 12, (2017) 132.
[8] M. D. Feinstein, A. Andronikides, and E. Almeida: npj Nanophoton., 2, (2025).
[9] J. Yu, J. Kim, H. Chung, J. Son, G. Boehm, M.A. Belkin, and J. Lee: Sci. adv., 11, (2025) eadw8852.
[10] Y. Liu, K. Xu, X. Fan, X. Wang, X. Yu, W. Xiong, and H. Gao: OEA, 7, (2024) 230108.
[11] J. Lee, N. Nookala, J.S. Gomez-Diaz, M. Tymchenko, F. Demmerle, G. Boehm, M.-C. Amann, A. Alù, and M.A. Belkin: Adv. Opt. Mat., 4, (2016) 664.
[12] X. Xu, P. Chen, T. Ma, J. Ma, C. Zhou, Y. Su, M. Lv, W. Fan, B. Zhai, Y. Sun, T. Wang, X. Hu, S.-N. Zhu, M. Xiao, and Y. Zhang: Nano lett., 24, 1303 (2024).
[13] P. Chen, X. Xu, T. Wang, C. Zhou, D. Wei, J. Ma, J. Guo, X. Cui, X. Cheng, C. Xie, S. Zhang, S. Zhu, M. Xiao, and Y. Zhang: Nat. comm., 14, (2023) 5523.
[14] S. Won, S. Choi, T. Kim, B. Kim, S.-W. Kim, and Y.-J. Kim: Nanophotonics, 12, (2023) 3373.
[15] L. Ackermann, C. Roider, K. Cvecek, N. Barré, C. Aigner, and M. Schmidt: Sci. rep., 13, (2023) 10338.
[16] R.W. Boyd: "Nonlinear optics", (Elsevier AP Academic Press, London, 2020) p. 74.
[17] J.W. Goodman: "Introduction to Fourier optics", (McGraw-Hill, New York, London, 1996) p. 57.
[18] F. Träger: "Springer handbook of lasers and optics: With 136 tables", (Springer, New York, 2007) p. 124.
[19] R. W. Gerchberg and W. O. Saxton: Optik, (1972) 35.
[20] X.-L. Liu, X. Lu, X. Liu, L.-B. Feng, J.-L. Ma, Y.-T. Li, L.-M. Chen, Q.-L. Dong, W.-M. Wang, Z.-H. Wang, Z.-Y. Wei, Z.-M. Sheng, and J. Zhang: Opt. lett., 36, (2011) 3900.
[21] S. Zheng, J. Tan, H. Liu, X. Lin, Y. Saita, T. Nomura, and X. Tan: OEA, 7, (2024) 230180.

(Received: June 30, 2025, Accepted: December 12, 2025)